Magnetism, Electronic State, and Local Structure of Iron-Containing Organometallic Polymers

Tadashi SUGANO, Masaharu NOMURA,† Kunio AWAGA, POH Lee Kieng,††
Toshiaki OHTA,† and Minoru KINOSHITA*
The Institute for Solid State Physics, The University of Tokyo, Roppongi, Minato-ku, Tokyo 106
†Photon Factory, National Laboratory for High Energy Physics, Ooho-machi, Tsukuba, Ibaraki 305
(Received March 10, 1986)

Schiff-base polymers were synthesized by the reaction of 2,6-pyridinedicarbaldehyde with 1,4-butane-, 1,6-hexane-, 1,8-octane-, and 1,12-dodecanediamine. Each of the polymers, when combined with iron(II) sulfate or iron(II) chloride, exhibited anomalously large magnetization and a nonlinear relation of the magnetization curve at room temperature. These iron-containing solids were found to be amorphous and, hence, the local structures around the iron atoms in the compounds were determined by the measurements of Fe K-edge X-ray absorption spectra. It was found that the iron atoms were each surrounded by six nitrogen atoms with the almost equivalent distance of 1.93±0.02Å. This was consistent with a possible geometry in which the tridentate ligand moieties of the polymers were coordinated with the iron atoms in a ratio 2 : 1. It was also found from the results of X-ray photoelectron and Mössbauer spectroscopies that the iron atoms in the solid obtained from the reaction between poly(2,6-pyridinediylmethylidynenitrilohexamethylenenitrilomethylidyne) and iron(II) sulfate were in two valence states consisted of the high spin (S=5/2) irons(lII) which were responsible for the observed magnetism and the low-spin (S=0) irons(II) which gave no contribution to the magnetism.

It is of great interest to study the magnetism due to the transition-metal ions coordinated with organic ligands, because there are several organometallic compounds exhibiting ferromagnetic behavior: Bis(diethyldithiocarbamato)iron(III) chloride, T_C=4.5 K;[1,2] bis(diethyldithiocarbamato)iron(III) bromide, T_C= 1.52 K;[3] and manganese(II) phthalocyanine, T_C= 8.6 K,[4,5] where T_C is the Curie temperature. Since the magnetic interactions among metal ions are expected to be controlled by varying the structure of ligands, the length of the repeating unit of polymer chains and the kind of metal ions, there may be a possibility of finding ferromagnetic organometallic compounds with a higher T_C.

Previously, we have shown that, when the organic polymer poly(2,6-pyridinediylmethylidynenitrilohexamethylenenitrilomethylidyne) $(C_{13}H_{17}N_3)_n$ is combined with iron(II) sulfate, a solid (abbreviated as **6**-SO_4) of which the chemical composition is approximately $[Fe(C_{13}H_{17}N_3)_2]SO_4 \cdot 6H_2O$ is obtained.[6,7] This solid shows an anomalously large magnetization over the whole temperature range from 1.9 to 300 K and S-shaped magnetization curves below about 50 K.[7] In order to obtain a further insight into this magnetism, we have synthesized new compounds in which the structure of the ligand moiety and the length of the methylene chain of the polymer are varied systematically from **6**-SO_4. In addition, since all the iron-containing solids obtained have been found to be amorphous, we have measured X-ray absorption spectra in order to determine the local structure around the iron atoms in the solids. Furthermore, to reveal the valence and spin states of the iron ions in the solids, we have examined the X-ray photoelectron and ^{57}Fe Mössbauer spectra of **6**-SO_4 and found that the iron ions in this solid contribute only partially to the magnetism.

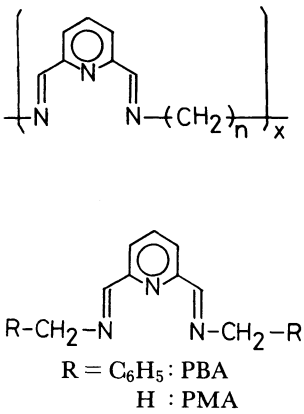

Fig. 1. Molecular structure of polymeric (a) and monomeric (b) ligands.

The present paper describes the applied field dependence of the magnetization of the iron-containing solids, the bond length and the coordination number around the iron atoms as well as their valences and spin states. The magnetic behavior of the solids will be discussed in relation to the structural and electronic properties derived from the results of X-ray absorption, X-ray photoelectron, and ^{57}Fe Mössbauer spectroscopies.

Experimental

The polymers shown in Fig. 1(a) were synthesized by the reaction of 2,6-pyridinedicarbaldehyde with 1,4-butane-, 1,6-hexane-, 1,8-octane-, and 1,12-dodecanediamine as described in the literature[6] and are abbreviated, respectively, as **4**, **6**, **8**, and **12**, according to the number of methylene groups, n. The obtained polymers were white powders and had a tendency to become fibrous upon increasing the length, n, of the methylene chain. When the polymers were treated with iron(II) sulfate or iron(II) chloride in an aqueous solution

††On leave of absence from Department of Physics, University of Agriculture Malaysia, Serdang, Salangor, Malaysia.

under a nitrogen stream, dark-violet solids were obtained. The solids were filtered off and dried over diphosphorus pentaoxide and sodium hydroxide in a vacuum desiccator. The solids are given abbreviated names: For instance, **4**-SO_4 and **8**-Cl_2 denote, respectively, solids prepared by combining polymer **4** with iron(II) sulfate and polymer **8** with iron(II) chloride. Typical results for elemental analyses are as follows; Found: C, 45.31; H, 6.57; N, 12.55; S, 5.49; Fe, 8.52%; Calcd for $[\{Fe(C_{13}H_{17}N_3)_2\}(SO_4)_{1.15}\cdot 5H_2O]_n$ (**6**-SO_4): C, 45.46; H, 6.46; N, 12.33; S, 5.37; Fe, 8.13%. Found: C, 50.40; H, 7.13; N, 11.92; Cl, 12.22; Fe, 7.81%; Calcd for $[\{Fe(C_{15}H_{21}N_3)_2Cl_{2.4}5H_2O]_n$(**8**-$Cl_2$): C, 50.21; H, 7.30; N, 11.71; Cl, 11.86; Fe, 7.78%. The water content varied to a small extent from sample to sample and the molar ratio of the sulfate or chloride ions was a little larger than the stoichiometry expected for bivalent iron ions. The latter modification of the chemical composition will be discussed below in relation to the valence state of the iron atoms.

As a reference compound for X-ray absorption measurements, two iron(II) complexes of the ligands shown in Fig. 1(b) were prepared and two ferrites γ-Fe_2O_3 (maghemite) and Fe_3O_4 (magnetite) were freshly prepared and identified by means of powder X-ray diffraction. The two complexes, [2,6-bis(benzyliminomethylene)pyridine]iron(II) bromide and [2,6-bis(methyliminomethylene)pyridine]iron(II) iodide, are abbreviated as PBA–$FeBr_2$ and PMA–FeI_2, respectively.

Fe K-edge X-ray absorption spectra were measured on powder samples sandwiched between adhesive tapes by using the EXAFS facilities installed at the beam-line 10B in Photon Factory. Extended X-ray absorption fine structure (EXAFS) oscillations were extracted by removing a cubic spline background with four sections. Bond distances and coordination numbers were determined by a single-shell curve-fitting analysis with the theoretically evaluated phase shifts.[8–10]

The infrared spectra were measured with a Perkin-Elmer PE684 infrared spectrometer. X-Ray photoelectron spectra were measured with a McPherson ESCA36 electron spectrometer by employing Mg $K\alpha$ (1253.6 eV) as the stimulating radiation. The X-ray photoelectron spectra were measured on a powder sample mounted onto an aluminum plate using a double-sided adhesive tape. The binding energies of photoelectron peaks were calibrated against that of the Au $4f_{7/2}$ peak (83.8 eV) of a thin gold film evaporated onto a sample surface in the spectrometer.

Mössbauer spectra were measured with a Shimazu MEG-2 Mössbauer spectrometer on powder samples at 77 and 300 K. Isomer shifts, quadrupole splittings and internal fields were calibrated against the six hyperfine splitting peaks of an iron metal separately measured as a reference.

The magnetization was measured with a Faraday-type susceptometer constructed in combination with a JEOL electromagnet and a Cahn 2000 electromicrobalance in the field range 0.1—0.4 T at room temperature.

Local Structure around the Iron Atoms

It is difficult to determine the molecular structure of these iron-containing solids by means of X-ray diffraction because they are found to be amorphous. Therefore, we have attempted to determine particularly the molecular structure around the iron atoms which are responsible for the magnetism, using X-ray absorption spectroscopy. Figure 2 shows the first derivative curves of the Fe K X-ray absorption near-edge structure (XANES) spectra of the solids, an iron foil, the two ferrites, and the monomeric iron(II) complexes. The spectra of the solids resemble those of monomeric complexes; this indicates that the local structures of iron-containing solids and the complexes are similar to each other. On the other hand, structures denoted by B or C split into two peaks in the spectra of the ferrites. Structure A, appearing in the pre-edge region, is attributed to quadrupolar-allowed 1s→3d transitions.[11] Its relative intensity is known to be weak for six-coordinated iron compounds, whereas it is strong for four-coordinated iron compounds.[12] The relative intensities of structure A of the iron-containing solids and complexes are similarly weaker than those of ferrites having four- and six-coordinated iron sites. Therefore, taking the chemical structure of the ligands into account, we could suggest that the iron atoms in the solids as well as those in the complexes are surrounded by six nitrogen atoms.

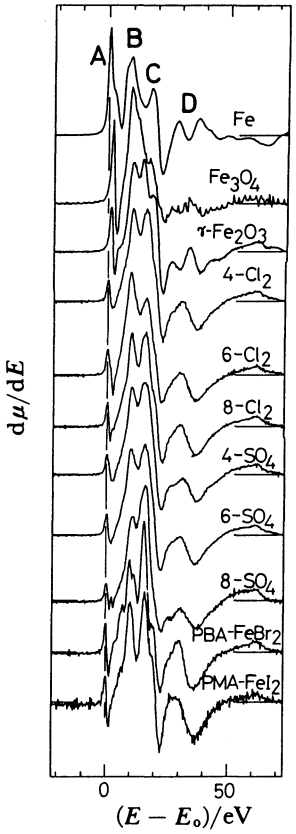

Fig. 2. First derivative $d\mu/dE$ curves of XANES spectra of an iron foil, ferrites the iron-containing solids, and the iron(II) complexes, where E is the photon energy and E_0 is the photon energy at the first maximum for the iron foil. The substances are given in abbreviated names (see the text).

Figure 3 shows a comparison among the EXAFS oscillations of iron, maghemite γ-Fe_2O_3, the iron-containing solids **6**-SO_4 and **6**-Cl_2, and the complex PBA–$FeBr_2$. It can be clearly seen that the EXAFS

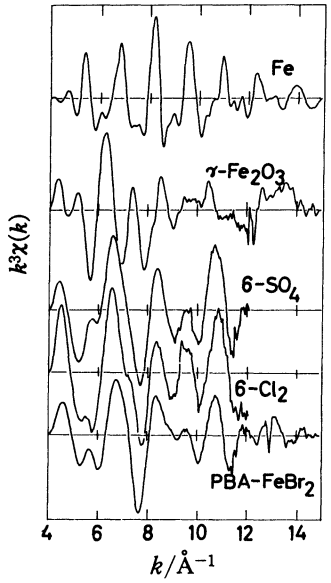

Fig. 3. EXAFS oscillations $k^3\chi(k)$ of the iron-containing solids and the iron(II) complexes.

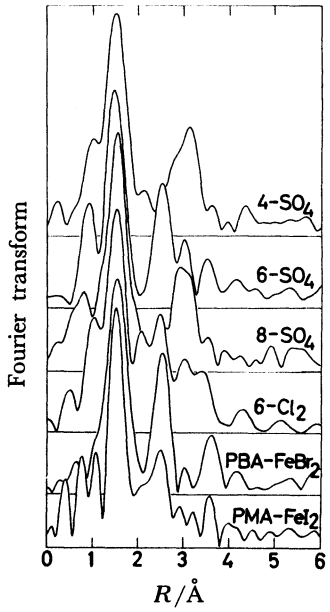

Fig. 4. Fourier transforms of EXAFS oscillations of the iron-containing solids and the iron(II) complexes.

oscillations of the solids are nearly identical to those of the complex, while they are very different from those of iron and maghemite. This behavior is quite similar to that observed in XANES spectra.

The Fourier transforms of the EXAFS oscillations, $k^3\chi(k)$ are shown in Fig. 4. The transforms for the iron-containing solids also resemble those for the complexes. The most prominent peak for the solids is located at about 1.5 Å (phase shift has not yet been corrected) and is coincident with the peak position for the complexes. This indicates that the peak corresponds to Fe–N bonds. From the chemical structure of the ligands, the peak at 2.5—3 Å could be due to Fe–C bonds.

We carried out a least-squares curve-fitting analysis by making a back-Fourier transformation of the region around the most prominent peak since it was difficult to construct reasonable structural models for second- and third-nearest neighbor atoms. The obtained bond distances are summarized in Table 1. The bond distances of the iron-containing solids are very similar to each other and are equal to those of the reference complexes within the experimental errors. Since the Fe–N bond distances in the six-nitrogen coordinated iron(II) complexes with ligands of similar molecular structure are known to be 1.9—2.0 Å,[13,14] the bond distance of 1.93±0.02 Å obtained for the iron-containing solids and the reference complexes are quite consistent with the Fe–N bond formation as expected from the molecular structure of the ligand moieties of the polymers.

The coordination number was shown to be about six for the reference complexes, although the estimated errors are somewhat large. This indicates that the present analysis which utilizes theoretical values of the phase shift instead of the experimental values is not

Table 1. The Fe–N bond Distance R and the Coordination Number N Derived from the Analysis of Fe K-edge EXAFS

Compound	R/Å (±0.02)	N (±1.0)
Monomer		
PBA-$FeBr_2$	1.93	5.9
PMA-FeI_2	1.90	5.8
Polymer		
4-SO_4	1.93	6.0
6-SO_4	1.94	5.3
8-SO_4	1.93	6.0
4-Cl_2	1.94	5.1
6-Cl_2	1.92	4.8
8-Cl_2	1.93	4.5

unreasonable for a determination of the coordination numbers for the compounds studied here. As shown in Table 1, the coordination numbers for the iron-containing SO_4-solids were found to be in the range from five to six. Although those for the Cl_2-solids are in the vicinity of five, these values seem to be underestimated to some extent in view of the similarity of the XANES and EXAFS spectra observed with all the solids and with the reference complexes. Therefore, it may be reasonable to conclude that the coordination numbers for these solids are six.

The above conclusion is further supported by the following fact. We have synthesized a polymer by reacting 1,6-hexanediamine with 1,3-benzenedicarbaldehyde instead of 2,6-pyridinedicarbaldehyde. This polymer is obtained as transparent soft lumps. We have tried to make a chelate compound of this polymer with iron(II) sulfate and chloride, but it turns out that the

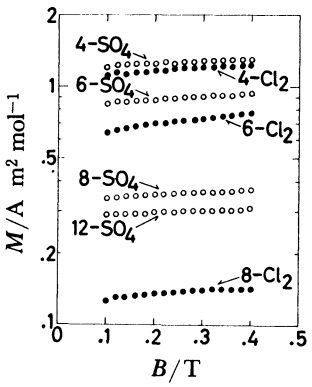

Fig. 5. Molar magnetization M of the iron-containing solids as a function of applied field strength B at room temperature.

polymer does not react with either sulfate or chloride. This implies that the tridentate structure of the ligand moiety is necessary for the polymer to form a chelate compound like **6**-SO_4; that is, the coordination number for the solids is six rather than four.

From the results mentioned above, it is concluded that the iron atoms in the solids are each surrounded by six nitrogen atoms with an almost equal distance of 1.93±0.02 Å, as observed for the iron(II) complexes in which one iron(II) ion is coordinated with two tridentate ligands. This conclusion is consistent with the 1:2 stoichiometry of Fe and the repeating units of the polymeric ligands determined by an elemental analysis. It is to be noted, at least from the results of X-ray absorption spectra, that there is no evidence for the presence of ferrite or metallic iron which would cause the ferromagnetism.

Effect of Chemical Modification of Polymers on the Magnetism

Since a magnetic interaction among the transition metal atoms is expected to be influenced by the chemical environment, particulary by the interatomic distances, we have examined the effect of chemical modifications of the length of the methylene chain and/or the anion on the magnetism of the iron-containing solids by comparing the magnetization curves at room temperature.

The length of the methylene chain does not qualitatively affect the magnetism. As shown in Fig. 5, all the iron-containing solids obtained by reacting polymers **4**, **6**, **8**, and **12** with iron(II) sulfate and iron(II) chloride exhibit magnetization curves similar to those of **6**-SO_4, i.e., a nonlinear relation to an applied field with a large magnetization, while the magnetization tends to decrease upon increasing the length, n, of the methylene chain. This indicates that only the tridentate structure is related to the large magnetization and its nonlinear relationship to the applied field.

The anions, sulfate and chloride, do not affect the magnetic behavior. Table 2 summarizes the molar magnetization of the iron-containing solids at 0.4 T. There seems to be a tendency to decrease the magnetization with a substitution of sulfate for a chloride ion. However, the magnitude of the magnetization still remains on the same order. The infrared spectra indicates that sulfate anions are only weakly or indirectly bound to the iron atoms. As shown in Fig. 6, the infrared spectrum of **6**-SO_4 exhibits the four bands attributable to sulfate ions at about 1100 cm^{-1} (ν_3) and at 610 cm^{-1} (ν_4) which are relatively strong in intensity and at 960 cm^{-1} (ν_1) and at 430 cm^{-1} (ν_2) which are very weak. Quite similar results have been obtained for all the solids containing sulfate ions. Since a free sulfate ion has a T_d symmetry, only a stretching mode (ν_3) and a bending mode (ν_4) are allowed for dipole transitions. This selection rule may be relaxed upon complex formation and the ν_1 and ν_2 modes appear with intensity, depending on the nature of the bonds formed. Simultaneously, each of bands due to ν_3 and ν_4 modes splits into two or three bands according to the occurrence of a symmetry lowering. The spectral feature observed is, therefore, characteristics of a sulfate ion that is very weakly bound to a metal ion.[15] On the other hand, a similar discussion may not be possible for monoatomic chloride anions.

Table 2. Molar Magnetization M/A m^2 mol^{-1} at 0.4 T and at 295 K of the Iron-Containing Solids Obtained by Reaction of the Polymers with $Fe^{II}SO_4$ or $Fe^{II}Cl_2$ (1 A M^2 mol^{-1} = 10^3 Oe emu mol^{-1})

Polymer	Anion	
	SO_4^{2-}	Cl^-
4	1.3 ±0.2	1.2 ±0.2
6	1.0 ±0.3	0.8 ±0.2
8	0.37±0.04	0.14±0.04
12	0.31±0.04	—

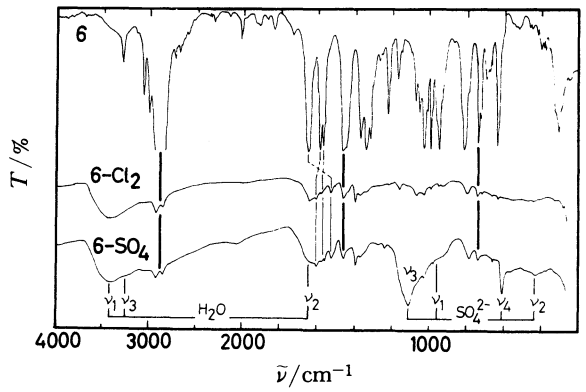

Fig. 6. Infrared spectra of **6**, **6**-SO_4, and **6**-Cl_2. The thick lines indicates the absorption bands assigned to the vibrational modes of the hexamethylene group of the polymer and the thin lines indicate those due to the tridentate moiety of the polymer. The vibrational modes of H_2O and those of SO_4^{2-} ion are also indicated. Similar results were obtained for the other polymers.

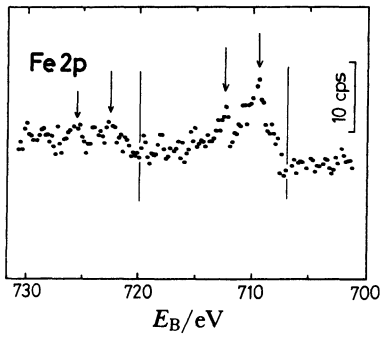

Fig. 7. Fe2p photoelectron spectrum of **6**-SO_4. Background is subtracted. The peak positions are indicated by arrows. Vertical lines represent the Fe2p peak position in metallic iron.

Table 3. Binding Energies of the Fe2p and N1s Core Electron Peaks in eV

Compound	$Fe2p_{1/2}$	$Fe2p_{3/2}$	N1s (fwhm)
6			399.3 (1.6)
6-SO_4	726	712.4	399.7 (2.3)
	723	709.5	
Fe-metal	720[b]	706.9[a]	
$Fe^{II}SO_4 \cdot 7H_2O$	723[b]	710.5[a]	
$[Fe^{II}(bpy)_3]SO_4$[c]	721.6[a]	709.2[a]	
$[Fe^{III}(oxinat)_3]$[d]		711.5[a]	
$(NH_4)_3[Fe^{III}F_6]$		713.8[a]	

a) Ref. 16. b) Ref. 17. c) Tris(2,2′-bipyridine)iron(II) sulfate. d) Tris(8-quinolinolato)iron(III).

However, as shown in Fig. 6, a close similarity of the infrared spectra due to tridentate moieties would exclude a strong coordination of the chloride ion with the iron. Therefore, the sulfate and chloride anions in the iron-containing solids are almost isolated from iron ions and, consequently, they do not affect the magnetism.

Valence and Spin States of the Iron Atoms

Since it is important to know the valence state of the iron species in the iron-containing solids in order to discuss their magnetic behavior, we have measured the X-ray photoelectron spectra of **6** and **6**-SO_4. Figure 7 shows the X-ray photoelectron spectrum of **6**-SO_4 in the Fe2p region. The signal-to-noise ratio is not very good since the atomic fraction of the iron in **6**-SO_4 is only one-ninetieth. However, two peaks can be recognized in the $Fe2p_{3/2}$ region; also, there seem to be two peaks in the $Fe2p_{1/2}$ region. The binding energies are listed in Table 3. The binding energies of all the peaks observed shift to the higher-energy side from those of metallic iron (Fig. 7). This suggests that the iron atoms are ionized in **6**-SO_4.

The lower energy side peak in the $Fe2p_{3/2}$ region is attributed to iron(II) since its bindigng energy is close to that of tris(2,2′-bipyridine)iron(II) sulfate[16] where the iron(II) ion is associated with the six nitrogen atoms and the SO_4^{2-} ion is separated from the iron(II) ion in good agreement to that of **6**-SO_4. The binding energy of the higher energy side peak is located between the binding energies[16] of $(NH_4)_3[Fe^{III}F_6]$ and tris(8-quinolinolato)iron(III), which are six-coordinate iron(III) complexes. Therefore, this peak can be ascribed to iron(III).

It is known that the photoelectron peaks of magnetic transition-metal compounds often accompany strong satellites at positions with binding energies higher by 4 to 6 eV.[18] The energy difference between the two peaks attributed to iron(II) and iron(III) is only 3 eV. Therefore, the high energy peak can not be regarded as a satellite of the low-energy peak. In addition, the results of Mössbauer measurements described below also suggest the presence of iron(III). Thus, it is quite reasonable to attribute the high-energy peak to iron(III).

Therefore, the irons in **6**-SO_4 are in the valence states of iron(II) and iron(III). **6**-SO_4 has been prepared by reacting **6** with iron(II) sulfate under a nitrogen stream to prevent the oxidation of the bivalent iron. It should be noted that **6**-SO_4 can not be obtained by a reaction between **6** and iron(III) sulfate. Therefore, the partial oxidation seems to occur after the iron(II) has been included in the polymer chains.

The presence of two valence states explains the nonstoichiometry of the sulfate ion in **6**-SO_4 described in the experimental section. It follows from the ratio of observed intensities of the peaks that about 70% of the iron ions is in the bivalent state and about 30% is in the tervalent state. To keep charge neutrality of **6**-SO_4, the chemical composition of the relevant part is written as $(Fe^{II}SO_4)_{0.7}[Fe^{III}(SO_4)_{1.5}]_{0.3}=Fe(SO_4)_{1.15}$. This composition agrees well with that obtained by an elemental analysis.

The N1s photoelectron spectra (not shown) of **6** and **6**-SO_4 exhibit a single peak without satellite. The binding energy shifts to the higher energy in **6**-SO_4. This energy shift implies that the formal charges on the nitrogen atoms become more positive in **6**-SO_4 than in **6**. This is consistent with the coordination of the iron with nitrogen. In addition, the full-width at half-maximum (fwhm) of the N1s peak is 1.6 eV for **6** and 2.3 eV for **6**-SO_4. The line broadening observed in the latter compounds would be related to the difference in the chemical nature of the nitrogen atoms which are coordinated with the iron.

The results discussed above clearly indicate that the irons in **6**-SO_4 are in the two valence states consisting of iron(II) and iron(III). Since no evidence has been found for the presence of a magnetic moment on the organic species in **6**-SO_4, it is natural to consider that the magnetic moment in **6**-SO_4 is associated with the iron ions.

Figure 8 shows the ^{57}Fe Mössbauer spectrum of **6**-SO_4 at 77 K. It is found from a Lorentzian least-squares curve fitting analysis that the experimental

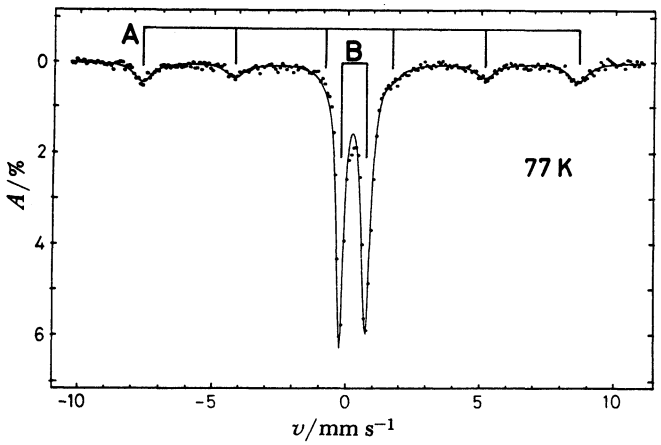

Fig. 8. Mössbauer spectrum of **6**-SO_4 at 77 K. Experimental points are shown by closed circles and the results of a Lorentzian least-squares fit is indicated by the solid line. The spectrum is composed of two subspectra denoted A and B. Stick diagrams indicate the peak positions of each subspectrum obtained by the analysis.

spectrum can well be reproduced by superimposing the subspectrum A which consists of six peaks of hyperfine splitting due to an internal field and the subspectrum B which consists of two peaks of quadrupole splitting. The absorption intensity of the Mössbauer spectra is markedly reduced at 300 K, probably due to a reduction of the recoil-free fraction. However, subspectra A and B still remain. The obtained parameters of the isomer shift δ, quadrupole splitting ΔE_q, and internal field H_i at 77 and 300 K are summarized in Table 4.

The subspectrum B can be attributed to the low-spin iron(II). The high-spin state (S=2) and the low-spin state (S=0) are possible for six-coordinate iron(II). The former possibility could be excluded on the basis of the values of the isomer shift. The isomer shift is known to be larger than 0.7 mm s^{-1} for a high-spin iron(II). Therefore, the iron(II) ions present in **6**-SO_4 have been concluded to be in a low-spin state. The iron(II) ions have no unpaired electrons in the low-spin state and, hence, does not cause an internal field. Therefore, subspectrum B should correspond to the low-spin iron(II). The quadrupole splitting of 0.96 mm s^{-1} obtained for the subspectrum B indicates the presence of an electric-field gradient induced by distortion from the octahedral symmetry, as is usually observed in low-spin iron(II) complexes with nitrogen donor ligands.[19]

On the other hand, the subspectrum A would be attributed to the high-spin state of iron(III). The presence of a hyperfine splitting in this subspectrum clearly indicates that the iron ion species have unpaired electrons. As discussed above, the possibility of high-spin iron(II) has already been eliminated. The remaining possibilities are, therefore, high-spin (S= 5/2) and low-spin (S=1/2) iron(III). These are not distinguishable from a difference in the isomer shift since the isomer shift is known to be comparable for

Table 4. Isomer Shift δ (relative to iron-metal film), Electric-Quadrupole Splittings ΔE_q, and Internal Field H_i Obtained from the Analysis of the Mössbauer Spectrum of **6**-SO_4 by the Lorentzian Least-Squares Curve Fitting

	77 K	300 K
Subspectrum A (Fe^{3+})		
δ/mm s^{-1}	0.46	0.46
ΔE_q/mm s^{-1}	−0.016	0
H_i/T	50.5±0.5	46±2
Subspectrum B (Fe^{2+})		
δ/mm s^{-1}	0.27	0.27
ΔE_q/mm s^{-1}	0.96	0.96

both states.[18] However, the internal field of 50.5±0.5 T is comparable with that of Fe_3O_4[20] and γ-Fe_2O_3[21] where iron(III) ions are in the high-spin state. In addition, this value is in good agreement with the internal field of 55 T expected for the $|M_S|$=5/2 state from the empirical relation for iron(III) ions in corundum, H_i=22$\langle S_z \rangle$.[22] Therefore, the assignment of the subspectrum A to the high-spin iron(III) is quite reasonable.

The fact that the quadrupole splitting observed for the subspectrum A is very close to zero also supports the above assignment. In the high spin-iron(III), the five d-electrons are separately distributed over the five d-orbitals so that the electron cloud becomes almost symmetric and the electric field gradient vanishes. It is known that the electron transfer between an iron atom and ligands is negligible in a high-spin iron compound[19] and that the electric field gradient is not affected very much by ligands.

The internal field is reduced to 46±2 T at 300 K, while the quadrupole splittings and the isomer shifts do not change. The reduction of internal field is quite natural, because the saturation magnetization decreases with increasing temperature.[7] A considerably large internal field, even at 300 K, indicates that the magnetic ordering would be maintained, even to a temperature higher than room temperature.

Concluding Remarks

From the discussion on the results of the X-ray photoelectron and Mössbauer spectroscopies, it is suggested that the iron atoms in **6**-SO_4 are in two valence states, consisting of the high-spin iron(III) which is responsible for the magnetism and the low-spin iron(II) which has no contribution to the magnetism. That is, only a fraction of the iron ions contributes to the observed magnetism in the iron-containing solids.

The large magnetization and its nonlinear relationship to an applied field was not only observed for **6**-SO_4 but also for the other iron-containing solids examined here. It was found that the length of the methylene chain of the polymer as well as the anions accompanying the iron ions hardly affect the

magnetism. Only the presence of the tridentate ligand moiety causes the formation of the iron-containing solids and, hence, the magnetism. This implies that the magnetic behavior observed for the iron-containing solids is not very much affected by the distance between the iron atoms coordinated with the tridentate moieties of the polymers, while the change in the length of the methylene chain may cause a variation of the distance.

This is somewhat peculiar for the large magnetization since magnetic interaction among the transition-metal ions may be influenced by their interatomic distances. X-Ray absorption measurements suggest that each of the iron ions in the solid is coordinated with two tridentate moieties of the polymers, as is expected for the stoichiometry determined by the elemental analyses. However, there remains a possibility of the presence of a small amount of iron ions which have different coordination characteristics and have escaped from observation because of limitations in the sensitivity of X-ray absorption spectroscopy for minor substances, including the same element.

The authors are greatful to Professor Takeshi Tominaga, Dr. Haruo Sato, and Dr. Motoyuki Matsuo for the measurements of the Mössbauer spectra. The authors also thank Professor Haruo Kuroda and Professor Isao Ikemoto for the use of the X-ray photoelectron spectrometer, and Professor Koichi Ohno for his valuable suggestions regarding this work.

This work was in part supported by the Grant-in-Aid for Scientific Research from the Ministry of Education, Science and Culture.

References

1) H. H. Wickman, A. M. Trozzolo, H. J. Williams, G. W. Hull, and F. R. Merritt, *Phys. Rev.*, **155**, 563 (1967).

2) G. E. Chapps, S. W. McCann, H. H. Wickman, and R. C. Sherwood, *J. Chem. Phys.*, **60**, 990 (1974).

3) S. Decurtins, F. V. Wells, K. C.-P. Sun, and H. H. Wickman, *Chem. Phys. Lett.*, **89**, 79 (1982).

4) C. G. Barraclough, R. L. Martin, S. Mitra, and R. C. Sherwood, *J. Chem. Phys.*, **53**, 1638 (1970).

5) H. Miyoshi, H. Ohya-Nishiguchi, and Y. Deguchi, *Bull. Chem. Soc. Jpn.*, **46**, 2724 (1973).

6) F. Lions and K. V. Martin, *J. Am. Chem. Soc.*, **79**, 2733 (1957).

7) T. Sugano, M. Kinoshita, I. Shirotani, and K. Ohno, *Solid State Commun.*, **45**, 99 (1983).

8) B. K. Teo, P. A. Lee, A. L. Simons, P. Eisenberger, and B. M. Kincaid, *J. Am. Chem. Soc.*, **99**, 3854 (1977).

9) P. A. Lee, B. K. Teo, and A. L. Simons, *J. Am. Chem. Soc.*, **99**, 3856 (1977).

10) M. Nomura, K. Asakura, U. Kaminaga, T. Matsushita, K. Kohra, and H. Kuroda, *Bull. Chem. Soc. Jpn.*, **55**, 3911 (1982).

11) A. Bianconi, "EXAFS for Inorganic Systems," Daresbury Laboratory, SERC DL/SCI/R17, 13 (1981).

12) G. Cales and J. Petieu, *Solid State Commun.*, **48**, 625 (1983).

13) V. L. Goedken, Y. Park, S.-M. Peng, and J. M. Norris, *J. Am. Chem. Soc.*, **96**, 7693 (1974).

14) A. Zalkin, D. H. Templeton, and T. Ueki, *Inorg. Chem.*, **12**, 1641 (1973).

15) K. Nakamoto, "Infrared and Raman Spectra of Inorganic and Coordination Compounds," 3rd ed John Wiley & Sons Inc., New York (1978).

16) L. Y. Johansson, R. Larsson, J. Blomquist, C. Cederstrom, S. Grapengiesser, U. Helgeson, L. C. Moberg, and M. Sundbom, *Chem. Phys. Lett.*, **24**, 508 (1974).

17) T. Tsang, G. J. Coyle, I. Adler, and L. Yin, *J. Electron Spectrosc. Relat. Phenom.*, **16**, 389 (1979).

18) L. Yin, I. Adler, T. Tsang, L. J. Matienzo, and S. O. Grim, *Chem. Phys. Lett.*, **24**, 81 (1974).

19) For example, N. N. Greenwood and T. C. Gibb, "Mössbauer Spectroscopy," Chappman and Hall Ltd., London (1971); H. Sano, "Mössubauer Spectroscopy: Application to Chemistry," (in Japanese) Kodansha Ltd., Tokyo (1972).

20) H. Weber and S. S. Hafner, *Z. Krist.*, **133**, 331 (1971).

21) J. M. Coey and D. Khalafalla, *Phys. Status Solidi A*, **11**, 229 (1972).

22) G. K. Wertheim and J. P. Remeika, *Phys. Lett.*, **10**, 14 (1964).